Title
A reassessment of HOx South Pole chemistry based on observations recorded during ISCAT 2000

Journal
Atmospheric Environment, 38(32)

ISSN
1352-2310

Authors
Chen, G
Davis, D
Crawford, J
et al.

Publication Date
2004-10-01

DOI
10.1016/j.atmosenv.2003.07.018

ELSEVIER

Atmospheric Environment 38 (2004) 5451–5461

ATMOSPHERIC ENVIRONMENT

www.elsevier.com/locate/atmosenv

A reassessment of HO_x South Pole chemistry based on observations recorded during ISCAT 2000

G. Chen[a,b,*], D. Davis[a], J. Crawford[b], L.M. Hutterli[c], L.G. Huey[a], D. Slusher[a], L. Mauldin[d], F. Eisele[d], D. Tanner[a], J. Dibb[e], M. Buhr[a], J. McConnell[f], B. Lefer[c], R. Shetter[c], D. Blake[g], C.H. Song, K. Lombardi[a], J. Arnoldy[a]

[a] *School of Earth and Atmospheric Sciences, Georgia Institute of Technology, Atlanta, GA, USA*
[b] *NASA Langley Research Center, Hampton, VA, USA*
[c] *Department of Hydrology & Water Resources, University of Arizona, Tucson, AZ, USA*
[d] *Atmospheric Chemistry Division, National Center for Atmospheric Research, Boulder, CO, USA*
[e] *Climate Change Research Center, Institute for the Study of Earth, Ocean, and Space, University of New Hampshire, Durham, USA*
[f] *Division of Hydrologic Sciences, Desert Research Institute, Reno, NV, USA*
[g] *Department of Chemistry, University of California, Irvine, CA, USA*

Received 3 October 2002; accepted 7 July 2003

Abstract

Reported here are modeling results based on ISCAT (Investigation of Sulfur Chemistry of Antarctic Troposphere) 2000 observations recorded at the South Pole (SP) during the Austral Summer of 2000. The observations included a comprehensive set of photochemical parameters, e.g., NO, O_3, and CO. It is worthy to note that not only were OH and HO_2 observed, but also HO_x precursor species CH_2O, H_2O_2, and HONO were measured. Previous studies have suggested that HONO is the major source of OH/HO_x in the Arctic; however, observed HONO levels at SP induced dramatic model overprediction of both HO_x and NO_x when used to constrain the model calculations. In contrast, model predictions constrained by observed values of CH_2O and H_2O_2 are consistent with the observations of OH and HO_2 (i.e., within 20%) for more than half of the data. Significant model overpredictions of OH, however, were seen at the NO levels lower than 50 pptv or higher than 150 pptv. An analysis of HO_x budget at the median NO level suggests that snow emissions of H_2O_2 and CH_2O are the single most important primary source of SP HO_x, contributing 46% to the total source. Major sinks for HO_x are found to be dry deposition of HO_2NO_2 and HNO_3 as well as their reactions with OH. Although ISCAT 2000 led to a major progress in our understanding of SP HO_x chemistry, critical aspects of this chemistry are still in need of further investigation.

Keywords: Antarctica; South Pole; Photochemistry; HO_x; Snow emissions; ISCAT

1. Introduction

It has long been recognized that free radicals are responsible for the tropospheric oxidation of most reduced trace gases emitted from natural as well as anthropogenic sources (e.g., Levy, 1974; Logan et al., 1981; Chameides and Davis, 1982; Thompson, 1992). Among the more important of these is the hydroxyl radical (OH). It largely controls the oxidizing power of the atmosphere. Yet another is the hydroperoxyl radical (HO_2), a product of many OH reactions. In the presence of nitric oxide (NO), rapid cycling between OH and HO_2

*Corresponding author. NASA Langley Research Center, Hampton, VA, USA.
E-mail address: gao.chen-1@nasa.gov (G. Chen).

1352-2310/$ - see front matter © 2004 Elsevier Ltd. All rights reserved.
doi:10.1016/j.atmosenv.2003.07.018

can enhance atmospheric OH through secondary production strengthening its dominance as the major tropospheric oxidizing agent. Because of this tight chemical linkage, the sum of HO_2 and OH is frequently abbreviated as HO_x. Studies focused on tropospheric HO_x sources and sinks are numerous and define one of the most important aspects of atmospheric chemistry (e.g., Crawford et al., 1999; Chen et al., 2001a, b; Jaegle et al., 2000,2001; Olson et al., 2001; Tan et al., 1998, 2001; Wang et al., 2001).

Our present understanding of HO_x chemistry indicates that at low altitudes production of HO_x is often proportional to UV solar radiation and H_2O levels. This naturally leads to an expected strong latitudinal gradient in OH. For example, both model results and field observations reveal that the tropics have some of the highest OH values to be found (e.g., Logan et al., 1981; Chamedies and Tan, 1981; Mauldin et al., 1999). For this reason, it was with great surprise that the first South Pole (SP) observations revealed OH levels whose summertime 24 h average was within 10% of the corresponding value in the tropics (Mauldin et al., 2001). Concomitant with these elevated OH levels were extraordinarily high mixing ratios (median, 225 pptv) of NO (Davis et al., 2001). These authors presented strong evidence suggesting the source of this SP NO being emissions from the snowpack, a by-product from the photolysis of nitrate. A modeling analysis of these ISCAT 1998 (Investigation of Sulfur Chemistry in Antarctic Troposphere) data by Chen et al. (2001b) showed that OH levels were a strong non-linear function of NO. The dominant source of OH was the recycling of HO_x through the reaction sequence $HO_2 + NO \rightarrow OH + NO_2$, followed by $OH + CO(O_2) \rightarrow HO_2 + CO_2$ (e.g., see Table 1 [R4] and [R3]). It was further shown that the largest primary source of HO_2 was photolysis of CH_2O [R13], the latter being a product from the OH initiated oxidation of CH_4 [R10]. Due to the high NO levels the amplification of HO_x through CH_4 oxidation was nearly a factor of 1.5 (i.e., HO_2 produced per OH consumed). The oxidation of CH_4, therefore, serves as a net source of HO_x, rather than a net sink as is typical of most remote boundary layer (BL) settings.

While the observed trends in NO, H_2O, O_3, and UV irradiance appeared to explain a large fraction of the ISCAT 1998 OH observations, a more detailed comparison of model predictions against observations exposed some shortcomings. Among these was the underprediction of OH at certain times. This has suggested the possibility of additional HO_x sources. Based on several Arctic studies, the additional sources were speculated to be the result of snowpack emissions of H_2O_2, CH_2O, and/or HONO (e.g., Dibb et al., 2002; Hutterli et al., 1999, 2001; McConnell et al., 1997; Sumner and Shepson, 1999; Zhou et al., 2001). Sensitivity tests by Chen et al. (2001b) showed that the photolysis of only very modest emissions of any of the above species could have provided the necessary primary source of HO_x. However, it was not possible to quantify these potential sources since no measurements were made.

Table 1
Summary of important photochemical reactions for SP HO_x

R1	$O_3 + h\nu \rightarrow O(^1D) + O_2$
R2	$O(^1D) + H_2O \rightarrow OH + OH$
R3	$OH + CO(O_2) \rightarrow HO_2 + CO_2$
R4	$HO_2 + NO \rightarrow OH + NO_2$
R5	$HO_2 + HO_2 \rightarrow H_2O_2$
R6	$H_2O_2 + h\nu \rightarrow OH + OH$
R7	$H_2O_2 + OH \rightarrow HO_2 + H_2O$
R8	$H_2O_2 \rightarrow$ RO/AS/DD[a]
R9	$OH + HO_2 \rightarrow H_2O + O_2$
R10	$OH + CH_4(O_2) \rightarrow CH_3O_2 + H_2O$
R11	$CH_3O_2 + NO(O_2) \rightarrow HO_2 + CH_2O + NO_2$
R12	$CH_2O + h\nu \rightarrow H_2 + CO$
R13	$CH_2O + h\nu(2O_2) \rightarrow 2HO_2 + HO_2 + CO$
R14	$CH_2O + OH + O_2 \rightarrow HO_2 + H_2O + CO$
R15	$CH_2O \rightarrow$ RO/AS/DD
R16	$OH + NO \rightarrow HONO$
R17	$HONO + h\nu \rightarrow OH + NO$
R18	$OH + HONO \rightarrow NO_2 + H_2O$
R19	$HONO \rightarrow$ RO/AS/DD
R20	$OH + NO_2 \rightarrow HNO_3$
R21	$HNO_3 + h\nu \rightarrow OH + NO_2$
R22	$OH + HNO_3 \rightarrow NO_3 + H_2O$
R23	$HNO_3 \rightarrow$ RO/AS/DD
R24	$HO_2 + NO_2 \rightarrow HO_2NO_2$
R25	$HO_2NO_2 + M \rightarrow HO_2 + NO_2 + M$
R26	$HO_2NO_2 + h\nu \rightarrow HO_2 + NO_2$
R27	$HO_2NO_2 + h\nu \rightarrow OH + NO_3$
R28	$HO_2NO_2 + OH \rightarrow H_2O + NO + O_2$
R29	$HO_2NO_2 \rightarrow$ RO/AS/DD

[a] RO = Rainout; AS = Aerosol scavenging; DD = Dry deposition.

From Chen et al.'s (2001b) analysis, it was also shown that the major HO_x loss pathways at SP are reactions of OH and HO_2 with NO_2 to form HNO_3 and HO_2NO_2. The final step in the loss process was speculated to involve mainly dry deposition of these acidic species (see Table 1, [R23] and [R29]) as well as, to a much lesser extent, reactions with OH ([R22] and [R28]); however, this was not confirmed since only very limited measurements of HNO_3 and none for HO_2NO_2 were obtained during the first ISCAT study.

ISCAT 2000 was carried out at Amundsen-Scott SP station, Antarctica during the months of November and December 2000. Quite significant in ISCAT 2000 though were the additional measurements of HO_2, H_2O_2, CH_2O, HONO, and HO_2NO_2. As a result, this paper has focused on re-examining current photochemical mechanisms applicable to the SP mixed layer, particularly the processes controlling the levels of HO_x.

2. Model descriptions

The model used in this study is the same as that employed in the ISCAT 1998 analysis. It is a time dependent box model containing explicit HO_x–NO_x–CH_4 chemistry (71 reactions) and parameterized NMHC chemistry (184 reactions). The latter chemistry has been significantly modified from the CAL scheme reported by Lurmann et al. (1986) (see e.g., Crawford et al., 1999). Typical model inputs consist of NO, CO, O_3, H_2O, ambient temperature, and pressure. However, the model can also accommodate observational constraints based on measurements of OH, HO_2, HNO_3, HO_2NO_2, H_2O_2, CH_2O, and HONO. The photolysis coefficients used in the analysis are those derived from in situ actinic flux measurements (see Davis et al., 2004a). Since no diurnal UV flux variations occur at SP during the Austral summer (there are variations, however, due to shifts in the overhead O_3 column density), photochemical steady state was assumed for all model calculated species. As the lifetimes of HO_x species are quite short, i.e., $\sim$3 s for OH and $\sim$30–80 s for HO_2, this assumption is quite reasonable for both species. The first order rate for heterogeneous removal of soluble species was taken to be $9 \times 10^{-5}\,s^{-1}$, the best deposition loss rate estimate for HNO_3 and HO_2NO_2 by Slusher et al. (2002) based on ISCAT 2000 dataset. This value is about one order of magnitude higher than that used in the 1998 study, and is based on the 2000 measurements of HNO_3. If the current deposition loss rate were applied to the ISCAT 98 analysis, the model OH would decrease, on average, by nearly a factor of 1.5 and the median $P(O_3)$ would be reduced by $\sim$0.8 ppbv day^{-1}. Model uncertainty based solely on rate coefficient uncertainties has been evaluated based on Monte Carlo sensitivity calculations. The model HO_x uncertainty based on these calculations was estimated at 40%.

3. Results and discussion

A summary of the observational data recorded during ISCAT 2000, together with a description of the instrumental technique (e.g., sensitivity and calibration), are presented in Davis and Eisele, 2004. For further details concerning a specific measurement, the reader is encouraged to examine individual contributions to this special issue. For completeness, however, the typical total uncertainty (random plus systematic errors) assigned to observations of OH, HO_2, HNO_3, and HO_2NO_2 were in the 20–60% range depending on the S/N (signal to noise) ratio of a specific measurement.

The interpretive analysis of ISCAT 2000 HO_x observations was based on 4604 individual model runs. These runs were mostly derived from 10-min data averages of the observed parameters NO, O_3, H_2O, and several j values. In addition, values for CO and nonmethane hydrocarbons (NMHC) were interpolated from grab sample observations having a typical temporal resolution of 2 to 4 samples day^{-1}. (The authors note that the day-to-day variations in CO were typically less than 5% and NMHC levels were sufficiently low as to have a negligible effect on the HO_x results.) Among the 4604 model runs completed, 2455 of these had OH measurements and 199 had HO_2 data. However, coincident OH and HO_2 data were not available because the same instrument was used to measure both species such that these measurements could not be made simultaneously. In addition to the HO_x measurements, there were 754 and 1185 runs having measurements of CH_2O and H_2O_2, respectively. Both CH_2O and H_2O_2 observations were recorded at 1 m above the snow surface (Hutterli et al., 2004). The measurement of HONO was made near the surface and at 10 m above the surface (Dibb et al., 2004). However, only very limited observations were recorded at 10 m. It was this group of data at 10 m that was used to constrain the model for purposes of evaluating the impact of HONO on SP HO_x sources. Other than H_2O_2, CH_2O, and HONO, all data were collected at 10 m above the snow surface. Since the vertical mixing is typically weak in SP (Oncley et al., 2004), the H_2O_2 and CH_2O levels may be lower at 10 m. Estimates of the eddy-diffusion calculation indicate that for neutral conditions this minor difference in sampling heights could lead to 7% and 5% drops for H_2O_2 and CH_2O, respectively (also see Hutterli et al., 2004). One should expect larger drops for stable conditions, which is probably more prevalent in SP. This will be further examined in terms of their impact on HO_x later in the text. As related to the HO_2 observations, only the sum of the concentrations of HO_2, OH, CH_3O_2, and RO_2 (Mauldin et al., 2004) could be measured as the instrument was configured at SP. The HO_2 fraction of the total radical sum was estimated from model runs. The HO_2 fraction typically ranged from 69% to 78%, with a median of 75%.

3.1. Comparison of model results with observations

As stated earlier, a major goal of this study was to quantitatively re-evaluate sources and sinks of SP mixed layer HO_x under summertime conditions. In particular, this required our examining the magnitude of the HO_x source resulting from snow emissions of H_2O_2, CH_2O, and HONO. During ISCAT 2000, snow emissions significantly enhanced the measured levels of all these HO_x precursors (Dibb et al., 2004; Hutterli et al., 2004). Our standard model (gas phase chemistry only) can only predict less than 4%, 39%, and 5% of observed levels of H_2O_2, CH_2O, and HONO, respectively. Thus, assessing the effect of snow emission on SP HO_x levels requires model calculations constrained by the observed values of

these precursor species. The effect of snow emissions then can be estimated by comparing the constrained model results with those from the standard model. Finally, the results from both models are compared against the observations.

Fig. 1a shows observed OH values and model results from the standard model. Fig. 1a shows that both modeled and observed OH are strongly modulated by NO with peak values occurring at ~100 pptv of NO. It is also apparent that model values are generally lower, except for values of NO <40 pptv. Overall, the median ratio of model to observation (M/O) is 0.68. Following the same approach for HO_2, Fig. 1b shows that observed HO_2 values are also higher than those predicted by the model. (The smaller range of NO values plotted against HO_2 versus OH primarily reflects the limited number of ISCAT 2000 HO_2 observations.) Again, the median M/O ratio for HO_2 is about 0.65. These differences between model and observations appear to be modest in comparison with model and observation uncertainties of 40%, which suggests that the median model bias could be removed by significant shifts in some kinetic rate coefficients and/or HO_x measurement calibration factors. Alternatively, the model underprediction of HO_x could also indicate that the model either underestimates HO_x sources or overestimates its sinks.

To test the hypothesis that HO_x sources might be underestimated, the ISCAT 2000 observations of CH_2O, H_2O_2, and HONO were used to constrain the model. All three species have previously been identified at Arctic sites. In each case, it has been stated that the major sources of these species were emissions from the snowpack (e.g., Dibb et al., 2002; Hutterli et al., 1999, 2001; McConnell et al., 1997; Sumner and Shepson, 1999; Zhou et al., 2001). Fig. 2 shows HO_x from both observations and model calculations constrained by observed values of CH_2O, H_2O_2, and HONO. Two different constraint levels are shown here. At the first level, only CH_2O and H_2O_2 observations are used to constrain the model. At the second constraint level, all three species (CH_2O, H_2O_2, and HONO) are used to

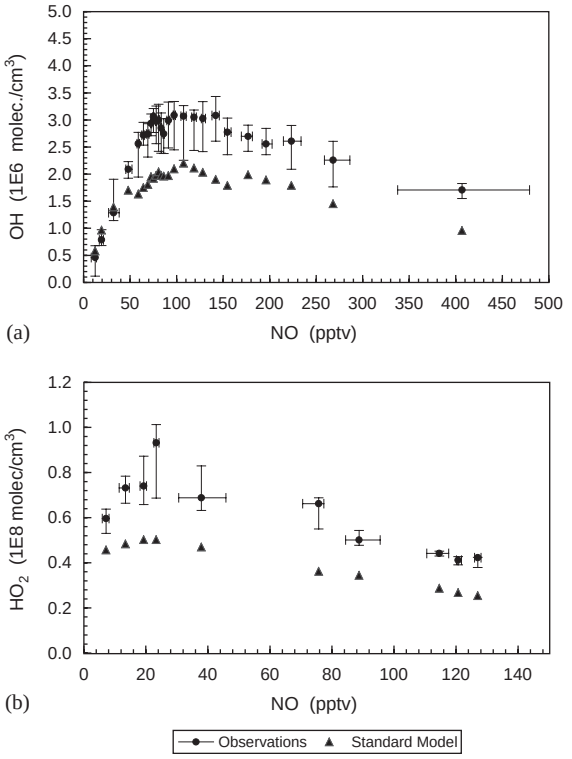

Fig. 1. Comparison of observations with standard model predictions for: (a) OH and (b) HO_2 as a function of NO. Each point in panel (a) represents the binned results from individual model runs or the average value from 10 min of observation. In each case 100 values have been used. In panel (b), each data point represents the binned results from only 20 values. Final values plotted are median values and the error bars indicate the lower and upper quartiles on the observational data. Standard model refers to the model with gas phase chemistry only.

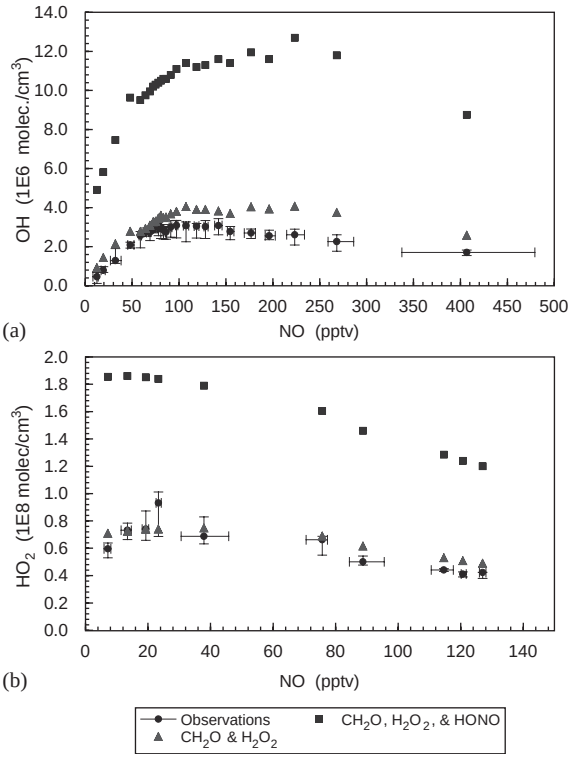

Fig. 2. Comparison of observations with constrained model predictions for: (a) OH and (b) HO_2 as a function of NO. Model and observational values have been derived in the same way as cited for Fig. 1.

constrain the model. It can be seen in the figures that constraining all three precursors leads to significant model overestimation of both OH and HO_2. The model values are factors of 2 to 3 and factors of 3 to 5 higher than observations of HO_2 and OH, respectively. At the median NO level of 89 pptv, the model predicted OH concentration approaches to 1.1×10^7 molec cm^{-3}.

Although direct measurements of OH have not been conducted at any Arctic sites, model estimates of OH based on HONO measurements are available for Summit, Greenland and Alert, Canada. It should first be noted, however, that the average SP HONO level is about a factor of 3–4 higher than that of Summit and a factor of 6 higher than the value measured at 5 m above surface in Alert. For springtime conditions at Alert, Zhou et al. (2001) suggested that production from HONO would increase peak OH values (noon) to 1.1×10^6 molec cm^{-3}. Based on observations at Summit, Yang et al. (2002) predicted noontime OH values approaching to 9×10^6 molec cm^{-3} in one case; however, the derived diel average was only $\sim 4 \times 10^6$ molec cm^{-3}. Although there are significant differences in the levels of other OH precursors between the SP and Arctic studies; the major factor driving the differences in model OH levels is most likely to be the in observed HONO levels.

In another assessment of the HONO observations, we examined the impact of HONO on the levels of NO_x, the rational being that HONO photolysis [R17] also serves as a source for NO. In fact, for periods of concurrent observation, NO values (at 10 m) and HONO values observed near the surface (85 cm) are positively correlated. This relationship can be well approximated by a second order polynomial with an R^2 value of 0.83. However, it is difficult to reconcile the observations of both of these species. For example, under the conditions of ISCAT 2000, the typical photochemical lifetime of HONO was only 7–10 min while that for NO_x was 7–25 h. Taking the average lifetime for each species and the median value of HONO sampled at 10 m (i.e., $\sim$26 pptv), the median NO_x level is predicted to be $\sim$10 times higher than what was observed. This raises the question of whether the measurement of HONO might suffer from some systematic error (e.g., chemical interference), although one can not rule out the possibility that the model mechanism might miss major HO_x and NO_x loss processes unique to the polar troposphere. While the mist chamber technique has been used in numerous studies involving various environmental conditions, there still exists the possibility of interference from any species that readily dissolves in aqueous solution to make nitrite. At this point, there are major difficulties in interpreting the HONO observations. Thus, we have focused our attention on the impact from snow emissions of CH_2O and H_2O_2 in the text that follows.

3.2. HO_x enhancement due to CH_2O and H_2O_2

Fig. 2 shows model results from calculations constrained by observed CH_2O and H_2O_2 levels. The constrained model HO_2 values are much closer to observations, as shown in Fig. 2b, than those from standard model. The median M/O ratio is 1.12. In the case of OH, however, median M/O ratio is 1.27 (1.22 for NO $<$130 pptv). Higher M/O ratios of $\sim$1.5 can be seen at NO values above 150 pptv. There are about 22% of model runs within this NO range. One of the contributing factors could be that the surface measurements of CH_2O and H_2O_2 could be too high for 10 m, the sampling height of OH and NO. Since there were no actual measurements available at 10 m, we have carried out sensitivity calculations with lowered the CH_2O and H_2O_2 by the estimated concentration drop (see discussions in Section 3) from 1 to 10 m. The corresponding decrease in M/O ratio for either OH or HO_2 is less than 3%. Since the larger model overestimations are at high NO levels and high NO levels are typically associated with meteorological stable conditions (Davis et al., 2004b), larger vertical gradient for both CH_2O and H_2O_2 can be expected for these conditions, which will, in turn, lead to greater reduction in M/O ratio. We do not believe, however, this difference in sampling heights will completely remove the model bias. Other explanations may involve one or a combination of factors, including missing HO_x loss processes, systematic model uncertainty in rate coefficients, and potential bias in observations of CH_2O, H_2O_2, and OH.

Despite the existing bias, constraining H_2O_2 and CH_2O does bring the model results closer to observations. In addition, it is necessary to constrain the model with observed CH_2O and H_2O_2 levels to better reflect the SP photochemical environmental conditions. As discussed earlier, Arctic studies have shown these two species to be important HO_x sources. To better understand the impact from snow emitted CH_2O and H_2O_2 on SP HO_x, here we present the results from a series of model sensitivity calculations to examine the HO_x sensitivities to H_2O_2 and CH_2O as well as their dependence on NO levels. The 4604 original model runs were divided into three groups according to the NO values: (1) runs where NO levels were in the lower 25th percentile of the distribution (i.e., 67 pptv); (2) runs having NO values within the inner quartiles; and (3) runs having NO values larger than the 75th percentile (i.e., 123 pptv). Three representative model runs were generated from these three NO groups by taking appropriate median values for model input parameters. These runs were then used in evaluation of the sources of CH_2O and H_2O_2 and their effect on SP HO_x.

Shown in Figs. 3a and b are the observed medians for H_2O_2 and CH_2O as well as predictions from the standard model which is based on gas phase chemistry

alone. Similar to other soluble species, the model assumes a dry deposition rate of $9 \times 10^{-5}\,s^{-1}$. The flux measurements by Hutterli et al. (2004) indicate that the snow, on average, is a net source of atmospheric H_2O_2 and CH_2O. But, it does not rule out dry deposition as a part of the air–snow exchange processes. The zero deposition case described by Hutterli et al. (2004) can be considered as a limiting case in which the emissions balance deposition. On average, the gas phase chemistry can only account for up to 3% and 30% of the observations of H_2O_2 and CH_2O, respectively. Even if the dry deposition rate is one order of magnitude smaller, it still leaves more than 70% of H_2O_2 and 30% of CH_2O observations unexplained. These results are consistent with those from a more detailed analysis by Hutterli et al. (2004). Together, the discrepancy between observations and model predictions based on gas phase chemistry alone argues that substantial amount of H_2O_2 and CH_2O are sustained by snowpack emissions. This is supported by CH_2O air–snow transfer model predictions (Hutterli et al., 2002) and by direct CH_2O and H_2O_2 flux measurements during ISCAT 2000. A comparison of those fluxes with the photochemical modeling can be found in Hutterli et al. (2004). Similar results were also reported by Hutterli et al. (1999, 2001) for analyses of CH_2O and H_2O_2 observations recorded at Summit, Greenland and by Sumner et al. (2002) for a CH_2O study in Alert, Nunavut, Canada.

To better understand the role of snow emissions, it is important to quantify how each of these emitted species influences HO_x levels. As noted earlier, sensitivity calculations were based on median conditions for low, mid, and high NO levels. The results of the sensitivity calculations are summarized in Fig. 4. Shown here are the observed medians for OH and HO_2, as well as the model predicted concentrations for these species based on four different constraint levels. Level 1 constraint represents the standard model (i.e., not constrained by either H_2O_2 or CH_2O); level 2 is constrained by H_2O_2 only; level 3 is constrained by CH_2O only; and level 4 shows the combined effects of being constrained by both H_2O_2 and CH_2O. From Fig. 4a, model predicted increases in OH from H_2O_2 only range from only 0.3 to $1.0 \times 10^6\,molec\,cm^{-3}$ (32–58%), while the corresponding HO_2 increase shown in Fig. 4b varies from 0.5 to $1.5 \times 10^7\,molec\,cm^{-3}$ (28–60%). In the case of constraining CH_2O only, from the lowest NO case to highest case, the model predict OH increase varies from 0.2 to $1.7 \times 10^6\,molec\,cm^{-3}$ (21–106%), while the corresponding HO_2 enhancement ranges from 1.2 to

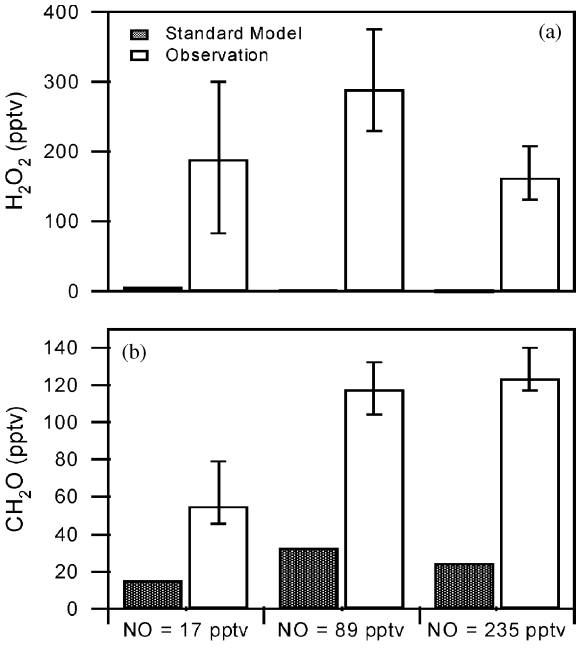

Fig. 3. Comparison of observations with standard model predictions for: (a) H_2O_2 and (b) CH_2O. The model calculations are based on representative runs derived from three data groupings defined by the NO concentration ranges. The observational bars are median values and the error bars on these denote the upper and lower quartile levels.

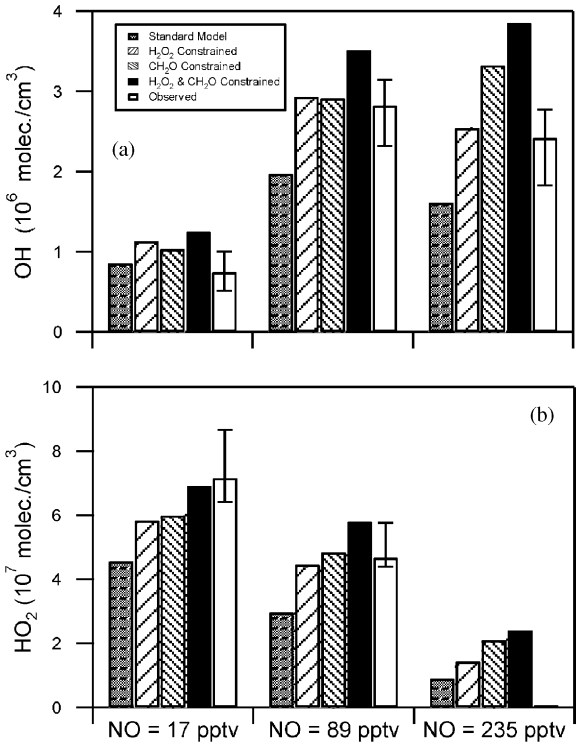

Fig. 4. Model estimated impact of snow emissions of CH_2O and H_2O on: (a) OH and (b) HO_2 and comparison with observations. Observational values are median values derived from the corresponding NO groups. Observational error bars represent inner quartile values.

1.9×10^7 molec cm^{-3} (31–134%). Considering that the observed levels of H_2O_2 are much higher than that of CH_2O, one can conclude SP HO_x is much more responsive to CH_2O than to H_2O_2 on a per-molecule basis. For example, the average OH sensitivities to H_2O_2 and CH_2O are 3.5×10^3 and 8.3×10^3 molec cm^{-3} pptv^{-1}, respectively. Even larger contrast can be seen in the case of HO_2, i.e., 0.5 vs. 1.7×10^5 molec cm^{-3} pptv^{-1}. A major reason for this is the difference in the photolysis rate for the two compounds. On average, CH_2O photolyzes nearly 5 times faster than for H_2O_2. Although not shown, the sensitivity calculations also reveal that the OH sensitivity is a strong function of NO, increasing by a factor of 4 from the lowest NO level to the highest as the partitioning of HO_x is shifted more favorably toward OH. Interestingly, the HO_2 sensitivity has a reverse dependence on NO levels, decreasing by a factor of $\sim$2.3 from the highest NO to the lowest reflecting the decrease in HO_x lifetime with increasing NO levels.

When the model is constrained by both H_2O_2 and CH_2O, the increase in OH and HO_2 levels, on average, is 17% less than that which would be estimated from taking the simple sum of the increases calculated independently for H_2O_2 and CH_2O. This 17% difference is partially due to the additional loss resulting from the reaction OH + HO_2 ([R7] see Table 1). The contribution from this reaction obviously would rapidly increase with HO_x level itself in a quadratic form. For the mid NO level case, there is a factor of $\sim$1.5 increase in this loss when comparing model constrained by both H_2O_2 and CH_2O with calculation constrained by only H_2O_2 or CH_2O. In addition to the loss increase, another important factor is the decrease in the net effect of snow emission on HO_x because of the enhancement in HO_x. For example, the net contribution from H_2O_2 to HO_x can be evaluated by Eq. (1):

$$P_{H_2O_2}(HO_x) = 2j_6[H_2O_2] - 2k_5[HO_2][HO_2], \quad (1)$$

where j_6 and k's are reaction rate coefficients. As shown in Eq. (1), for a given ambient concentration of H_2O_2 its contribution to HO_x is a quadratic function of HO_x level. Again for mid NO levels, $P_{H_2O_2}(HO_x)$ from the calculation constrained by both CH_2O and H_2O_2 is less than 60% of the value if only H_2O_2 is constrained. In the case of CH_2O, an equation similar to Eq. (1) can also be derived but is much more complicated due to the complexity of CH_4 chemistry. The net effect of CH_2O, however, has a much weaker dependence on HO_x level. Again for mid level NO case, the decrease in CH_2O contribution is only about 25%.

3.3. HO_x sinks

In Chen et al's. (2001b) 1998 ISCAT study, the authors suggested that the largest HO_x loss pathways involve the formation of HNO_3 and HO_2NO_2, i.e., reactions [R20] and [R24]. The role of HO_2NO_2 can be seen in the sequence of reactions [R25], [R26], [R27], [R28] and [R29] as shown in Table 1. The net HO_x loss can be estimated from Eq. (2):

$$k_{24}[HO_2][NO_2] + k_{28}[OH][HO_2NO_2] - (k_{25} + j_{26} + j_{27})[HO_2NO_2]. \quad (2)$$

It would appear that the thermal decomposition of pernitric acid ([R25]) might be one of the pivotal reactions of this sequence. This reaction can rapidly return HO_2 to the HO_x reservoir and yet the rate coefficient for this process, k_{25}, has one of the largest uncertainties associated with it at low temperatures (DeMore et al., 1997). This uncertainty has been estimated to be as large as a factor of 10 for SP summertime conditions. Sensitivity tests, however, have suggested that HO_x levels are relatively insensitive to the value of k_{25}. For a factor of 10 reduction in k_{25}, calculated HO_x levels decreased by 10% or less. Increasing k_{25} by the same factor, however, led to HO_x increases of up to 60%. Based on an analysis of NO_x and HO_2NO_2 observations, Slusher et al. (2002) suggested that the upper limit on the uncertainty of k_{25} should be no more than a factor of 3.3. In this case, the variation of HO_x driven by k_{25} would be less than 20%.

Heterogeneous losses of HO_x may also be quite important at SP (Chen et al., 2001b). During ISCAT 1998, observations suggested significant HO_2 scavenging frozen fog droplets on two occasions. A similar event occurred over the time period of 12–13 December during ISCAT 2000. At this time, the SP meteorological station recorded nearly 24 h of frozen fog and fog/misty conditions with visibility dropping from over 10 to $\sim$1 km. On this occasion, the NO level also dropped from an average of 175 pptv to less than 10 pptv. The photolysis rates jO(^1D) and j(NO_2) decreased by a factor of 1.3 and 1.5, respectively. The levels of CH_2O reduced from $\sim$140 to 35 pptv; while the H_2O_2 decreased from $\sim$250 to $\sim$75 pptv. And finally, OH values dropped from an average of 3×10^6–1.3×10^5 molec cm^{-3}. Unfortunately, there were no HO_2 values recorded during this time period.

As in ISCAT 1998, we believe that the cited shift in OH during ISCAT 2000 was caused by two factors: (1) a decrease in precursors, i.e., NO and, to a much lesser extent, H_2O_2 and CH_2O and (2) scavenging of HO_2 by fog droplets. The impact from dropping NO levels was addressed earlier in this text in Section 3.1 and is directly tied to the recycling of OH through reaction [R4]. Regarding the impact of fog droplets on HO_x, there have been field observations showing large HO_x decreases in clouds (e.g., Mauldin et al., 1998). Model sensitivity calculations showed a significant reduction in OH due to lower values of NO; however, these values

were still nearly a factor of 7 times higher than the observations for the time period corresponding to the on-set of ice-fog. Chen et al. (2001b) previously estimated a median value for heterogeneous loss of HO_2 of $9 \times 10^{-3}\,1\,s^{-1}$. This estimate was derived from a fog droplet size range of 5–10 μm having a number density of 5–15 cm^{-3}. Use of this HO_2 loss rate coefficient led to a decrease by factor of 3 for OH and a factor of 8 for HO_2. Although the model OH remains to be more than a factor of two higher than the observations, the difference is within the bounds of the combined uncertainty for both model and observations. Even further increase the HO_2 loss rate to the maximum value, the model OH decrease would be less than 20% while HO_2 reduction is proportional to its loss rate increase. This is because the HO_2 is already so low that the contribution from OH secondary formation (HO_2 reaction) is nearly negligible. Although addition of heterogeneous loss to the model has not reproduced the observations of OH, it is evident that the HO_2 heterogeneous loss may be quite important and requires further clarifications. The future study should include in-situ simultaneous observations of both OH and HO_2 as well as the number size distribution of SP fog droplets.

3.4. Assessment of HO_x budget

Fig. 5 summarizes the important SP HO_x photochemical processes. As discussed earlier in the text, the snow emissions of H_2O_2 and CH_2O must be included as HO_x sources not only in Arctic sites (e.g., Hutterli et al., 2001) but also in SP and possibly in other snow covered areas. Considering the sources and sinks shown in the figure, a HO_x budget analysis is carried out using the mid NO level (i.e., 89 pptv) condition as defined earlier in Section 3.2. It was noted here that the best agreement between model predictions and observations was found around this NO level (e.g., see Figs. 2a and b).

Summarized in Fig. 6a are the major sources of SP HO_x. The largest source is that labeled as 'Snow Emissions'. This source is made up of HO_x produced from the photolysis of snow released CH_2O and H_2O_2. They define ~32% and 14% of the total HO_x source, respectively. Next in line are CH_4 oxidation chemistry and O_3 photolysis. Both of these contribute ~27%. Of the total CH_2O contribution (snow + CH_4 oxidation), 54% is from snow emissions and 46% comes from CH_4 oxidation. Overall, therefore, snow emissions define the single largest source of SP HO_x (i.e. 46%). A comparison with the standard model output reveals that snow emissions lead to a factor of 2.3 increase in the total HO_x formation rate (vs. a factor 1.8 of in HO_x abundance). Similar results have been shown in the Arctic studies carried out in Alert, Canada and Summit Greenland (Yang et al., 2002; Hutterli et al., 2001). Finally, we would like to note that our sensitivity

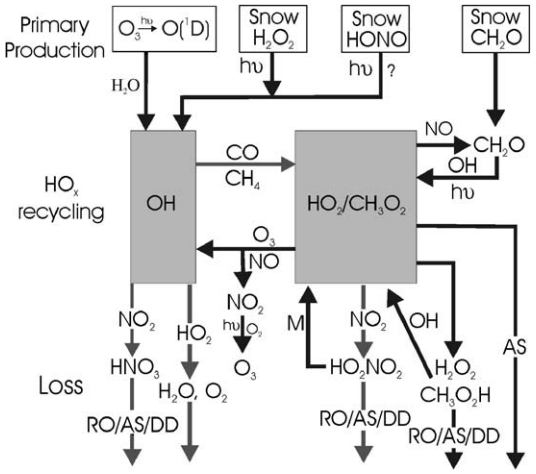

Fig. 5. Simplified HO_x–NO_x–CH_4 photochemical scheme reflecting SP summertime photochemistry. (Modified from Fig. 1. in Chen et al. (2001a, b).)

calculations suggest that for the case of zero deposition the snow emission would still make up 23% of the total HO_x production. In this case, CH_4 oxidation would be the largest HO_x source, contributing 50%; while the remainder 27% is the contribution from the reaction of $O(^1D) + H_2O$.

Major SP HO_x sinks are summarized in Fig. 6b. As presented in Section 3.3, the largest of these is the loss of HO_2 through the formation and subsequent deposition of HO_2NO_2 ([R29]). In addition, HO_2NO_2 can lead to further HO_x loss via its reaction with OH (e.g., [R28]). Together, these two HO_2NO_2 related HO_x loss pathways define ~45% of the total. The significant role of HO_2NO_2 in removing SP HO_x reflects the fact that HO_2NO_2 is reasonably stable due to low temperature and can be rapidly deposited to snow. The radical–radical reaction (i.e., $OH + HO_2$, [R9]) contributes another 30%. The final contribution comes from the reaction of OH with NO_2 to produce HNO_3, [R20], which then mainly undergoes deposition to the surface snow ([R23]). The latter process makes up the last 24% of the total HO_x sink. The above cited losses lead to an overall HO_x lifetime estimate of 5.8 min. By comparison, the lifetime estimated using the standard model is 6.8 min.

Significant differences exist in the estimated HO_x losses for ISCAT 2000 vs. ISCAT 1998. Chen et al. (2001a, b) suggested that the major HO_x loss (i.e., 62%) was through HNO_3 reactions ([R23] and [R22]). In ISCAT 2000, however, the major HO_x loss pathway was shown to be through HO_2NO_2 reactions. Furthermore, at the lower NO levels encountered in 2000 formation of HO_2NO_2 ([R13]) is more efficient than that of HNO_3

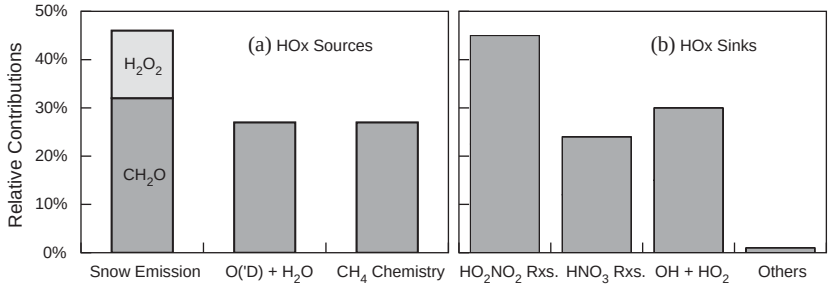

Fig. 6. HO_x budget analysis for SP summertime Photochemistry: (a) sources, (b) sinks. This analysis is based on the use of the mid NO case at 89 pptv.

([R42]) because of higher HO_2 level. As shown in Figs. 1b and 2b, the HO_2 concentration rapidly decrease with increasing NO levels. A close examination of the model results revealed that the HO_x loss through HO_2NO_2 is more important when NO levels are lower than $\sim$120 pptv. On the other hand, at a given NO level, our sensitivity test shows the HO_2 level is a strong function of the HO_x primary production (e.g., [R2]).

3.5. Implications to SP surface ozone

Crawford et al. (2001) has shown strong evidence suggesting surface photochemistry can play a significant role in modifying the SP surface ozone seasonal trend and generate late Spring/early Summer perturbations in O_3 level that exceeded the Winter maximum levels. These authors reported a median model estimated net ozone production rate of 2.8 ppbv day^{-1}. This production rate is equivalent to nearly 10% of average SP surface ozone concentration per day. Based on the observations from 2000, we have estimated the median net ozone production rate ($P(O_3)$) of 4.2 ppbv day^{-1} or nearly 13% per day. As shown in Fig. 7, the $P(O_3)$ is a strong non-linear function of NO level. The peak $P(O_3)$ value of $\sim$6.5 ppv day^{-1} situates around 160 pptv of NO and the inner quartile range was estimated to be from 3.2 to 4.8 ppbv day^{-1}. The higher values in 2000 can mainly be attributed to two factors: observed NO range and extra HO_x sources from snow emission of H_2O_2 and CH_2O. Recall the observed NO median for the 1998 study was 225 pptv (Davis et al., 2001) and the median derived from observations of 2000 is only 89 pptv. As shown by Crawford et al. (2001), the net ozone production rate has fallen to less than half of the peak value at 225 pptv of NO. By contrast, well over 73% of model runs for 2000 data give $P(O_3)$ values larger than the half of the peak value of $\sim$6.5 ppbv day^{-1}. The non-monotonic relation between $P(O_3)$ and NO has been discussed by Crawford et al. (2001). These authors have shown the linkage the intensity of photochemistry with the magnitude of $P(O_3)$. This can be also seen here by

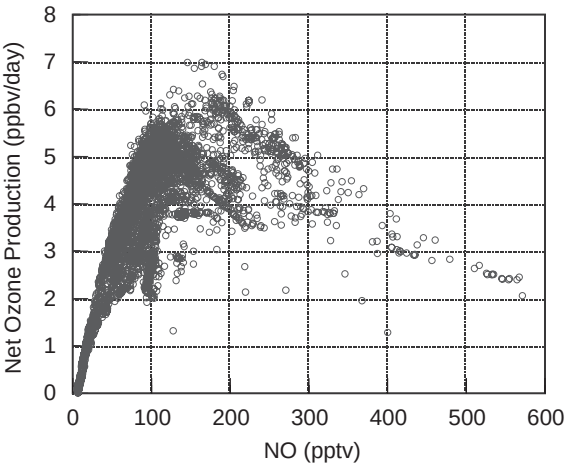

Fig. 7. Model calculated net O_3 production vs. observed NO for SP during ISCAT 2000.

comparing the Figs. 1 and 2 with Fig. 7. In fact, the $P(O_3)$ and model predicted OH is highly correlated with an R^2 value of 0.97. This is because both $P(O_3)$ and OH levels are largely controlled by the reaction of HO_2 with NO.

Generally, the $P(O_3)$ trend closely mimics that of the gross ozone production rate ($F(O_3)$). This reflects the fact that the photochemical ozone destruction rate ($D(O_3)$), on average, is less than 18% of $F(O_3)$ values. The major ozone production channel is the reaction of $HO_2 + NO$, contributing nearly 80% of total. The remainder is through the $CH_3O_2 + NO$ reaction. The two largest O_3 destruction pathways are the reactions of $OH + O_3$ and $HO_2 + O_3$, constituting $\sim$46% and $\sim$23% of the total, respectively. The relative importance of these two processes can be understood by the low HO_2/OH ratio of $\sim$16 and the enhanced reaction rate coefficient difference of a factor of 33, resulting from the SP environmental conditions characterized by low temperature and high NO levels. The reaction of $O(^1D) + H_2O$ makes up a mere 12% due to the dryness

of SP. The remaining 18% of ozone loss is through a sequence of reactions starting from $NO + O_3$ and followed by $NO_2 + OH$.

4. Summary and conclusions

The OH levels recorded in ISCAT 2000 now place the average 24 h oxidizing capacity of near surface air at SP to be larger than that in the tropical marine BL. The current analysis of SP HO_x chemistry has provided strong evidence that SP HO_x levels not only have a strong dependence on snow emissions of NO but also on emissions of CH_2O and H_2O_2. Both compounds were found to be present at SP at levels much higher than those predicted based on gas phase photochemistry alone. The model analysis suggests that the observations of HONO are inconsistent with both the observations of HO_x and NO. The difference between observations and model predications far exceeds the limits defined by the combined uncertainties for the model and observations. By contrast, constraining the model with observed values of CH_2O and H_2O_2 leads to model predicted HO_x levels that are well within the aforementioned uncertainties. Our results related to HONO would appear to be in conflict with those found at Summit Greenland and at other Artic polar sites where HONO has been identified as the major OH source. On the other hand, it must be recognized that no direct observations of OH were available at these Arctic sites to test their conclusions.

A HO_x budget analysis has revealed that snow emissions of CH_2O and H_2O_2 may constitute the single largest HO_x source at SP. The total contribution is estimated at 46%, 32% of which could be assigned to CH_2O and 14% to H_2O_2. The other important sources are identified as CH_4 oxidation chemistry and O_3 photolysis (i.e., $O(^1D) + H_2O$), each contributing $\sim$27%. The greater efficiency of CH_2O in its influence on HO_x levels primarily reflects the five times higher photolysis rate of CH_2O. Over 93% of the impact from H_2O_2 is estimated to come from snow emissions of this species. In contrast, only 60% of the impact from CH_2O is from snow emissions, with the remainder coming from CH_4 oxidation chemistry.

The analysis of SP HO_x sinks indicates that the largest sink is through the reaction [R24], $HO_2 + NO_2$ (45%), followed by HO_2NO_2 dry deposition and reaction with OH ([R27] and [R26]). The second largest sink involves the radical–radical reaction, $OH + HO_2$ (e.g., 30% of the total). Loss of HO_x through HNO_3 contributes $\sim$24%. The relative importance of HO_x loss through HO_2NO_2 vs. HNO_3 is primarily dictated by the ambient NO level.

It is evident that additional polar studies of HO_x chemistry will be required. Having available simultaneous observations of HO_2 and OH will be a critical need. Obviously, a resolution of the importance of HONO as a source of OH and NO_x will also be critical. The latter will require new specific measurement techniques for HONO as well as a reassessment of model HO_x sink processes.

Acknowledgements

The authors would like to acknowledge that this research is partially supported by the NSF office of Polar programs and the Division of Atmospheric Chemistry through Grant ♯OPP-9725465. The authors would also like to thank NOAA's CMDL group for making available SP O_3, CO, and meteorological data and the Raytheon staff for helping us make this field mission a successful one. Of particular significance are the contributions from Mr. Dana Hrubes.

References

Chameides, W.L., Davis, D.D., 1982. Chemistry in the troposphere. Chemical and Engineering News 60, 38–52.

Chamedies, W.L., Tan, A., 1981. The two-dimensional diagnostic model for tropospheric OH: an uncertainty analysis. Journal of Geophysics Research 86, 5209–5223.

Chen, G., et al., 2001a. An assessment of HO_x chemistry in the tropical Pacific boundary layer: comparison of model simulations with observations recorded during PEM tropics A. Journal of Atmospheric Chemistry 38, 317–344.

Chen, G., et al., 2001b. An investigation of South Pole HO_x chemistry: comparison of model results with ISCAT observations. Geophysical Research Letters 28, 3633–3636.

Crawford, J., et al., 1999. Assessment of upper tropospheric HO_x sources over the tropical Pacific based on NASA GTE/PEM data: net effect on HO_x and other photochemical parameters. Journal of Geophysical Research 104, 16255–16273.

Crawford, J., et al., 2001. Evidence for photochemical production of ozone at the South Pole surface. Geophysical Research Letters 28, 3641–3644.

Davis, D., et al., 2001. Unexpected high levels of NO measured at South Pole. Geophysical Research Letters 28, 3625–3628.

Davis, D., Eisele, F., Chen, G., et al., 2004a. Overview of ISCAT 2000. Atmospheric Environment, 2004, this issue, doi:10.1016/j.atmosenv.2004.05.037.

Davis, D., et al., 2004b. South Pole NO_x chemistry: an assessment of factors controlling its variability and absolute levels. Atmospheric Environment, 2004, this issue, doi:10.1016/j.atmosenv.2004.04.039.

DeMore, W.B., et al., 1997. Chemical kinetics and photochemical data for use in stratospheric modeling, evaluation number 12. Technical Report JPL Publication 97-4, NASA Jet Propulsion Laboratory.

Dibb, J.E., Arsenault, M., Peterson, M.C., Honrath, R.E., 2002. Fast nitrogen oxide photochemistry in Summit, Greenland snow. Atmospheric Environment 36 (15–16), 2501–2511.

Dibb, J.E., Huey, L.G., Slusher, D.L., Tanner, D.J., 2004. Soluble reactive nitrogen oxides at South Pole during ISCAT 2000. Atmospheric Environment, 2004, this issue, doi:10.1016/j.atmosenv.2003.01.001.

Hutterli, M.A., Rothlisberger, R., Bales, R.C., 1999. Atmosphere-to-snow-to-firn transfer studies of HCHO at Summit, Greenland. Geophysical Research Letters 26, 1691–1694.

Hutterli, M.A., McConnell, J.R., Stewart, R.W., Jacobi, H.-W., Bales, R.C., 2001. Impact of temperature-driven cycling of hydrogen peroxide (H_2O_2) between air and snow on the planetary boundary layer. Journal of Geophysics Research 106 (D14), 15395–15404.

Hutterli, M.A., Bales, R.C., McConnell, J.R., Stewart, R.W., 2002. HCHO in Antarctic snow: preservation in ice cores and air–snow exchange. Geophysics Research Letter 29 (8), 10.1029/2001GL014256.

Hutterli, M., et al., 2004. Formaldehyde and hydrogen peroxide in air, snow, and interstitial air at South Pole. Atmospheric Environment, 2004, this issue, doi:10.1016/j.atmosenv.2004.06.003.

Jaegle, L., et al., 2000. Photochemistry of HO_x in the upper troposphere at northern midlatitudes. Journal of Geophysical Research–Atmospheres 105, 3877–3892.

Jaegle, L., et al., 2001. Chemistry of HO_x radicals in the upper troposphere. Atmospheric Environment 35, 469–489.

Levy, H., 1974. Photochemistry of the troposphere. Advances in Photochemistry, Vol. 9. Wiley, New York, pp. 369–524.

Logan, J., et al., 1981. Tropospheric chemistry: a global perspective. Journal of Geophysical Research 86, 7210–7254.

Lurmann, F.W., Lloyd, A.C., Atkinson, R., 1986. A chemical mechanism for use in long-range transport/acid deposition computer modeling. Journal of Geophysical Research 91, 10905–10936.

Mauldin, R.L., Frost, G.J., Chen, G., Tanner, D.J., Prevot, A.S.H., Davis, D.D., Eisele, F.L., 1998. OH Measurements during the first aerosol Characterization Experiment (ACE 1): observations and model comparisons. Journal of Geophysical Research 103, 16713–16729.

Mauldin, R.L., Tanner, D.J., Eisele, F.L., 1999. Measurements of OH during PEM-Tropics A. Journal of Geophysical Research–Atmospheres 104, 5817–5827.

Mauldin, R.L., et al., 2001. Measurements of OH aboard the NASA P-3 during PEM-Tropics B. Journal of Geophysical Research–Atmospheres 106, 32657–32666.

Mauldin, R.L., et al., 2004. Measurement of OH, HO_2/RO_2, H_2SO_4, and MSA during ISCAT 2000. Atmospheric Environment, 2004, this issue, doi:10.1016/j.atmosenv.2004.06.031.

McConnell, J.R., et al., 1997. Physically based modeling of atmosphere-to-snow-to-firn transfer of hydrogen peroxide at South Pole. Journal of Geophysical Research 103, 10561–10570.

Olson, J.R., et al., 2001. Seasonal differences in the photochemistry of the South Pacific: a comparison of observations and model results from PEM-Tropics A and B. Journal of Geophysical Research–Atmospheres 106, 32749–32766.

Oncley, S., Buhr, M., Lenschow, D., Davis, D., Semmer, S., 2004. Observations of summertime NO fluxes and boundary-layer height at the South Pole using scalar similarity. Atmospheric Environment, 2004, this issue, doi:10.1016/j.atmosenv.2004.05.053.

Slusher, D.L., et al., 2002. Measurements of Pernitric Acid at the South Pole During ISCAT 2000. Geophysical Research Letters 29 (21), 2011, 10.1029/2002GL015703.

Sumner, A., Shepson, P., 1999. Snowpack production of formaldehyde and its impact on the Artic Troposphere. Nature 398, 230–233.

Sumner, A.L., et al., 2002. Atmospheric chemistry of formaldehyde in the Arctic troposphere at Polar Sunrise, and the influence of the snowpack. Atmospheric Environment 36 (15–16), 2553–2562.

Tan, D., et al., 1998. In situ measurements of HO_x in aircraft exhaust plumes and contrails during SUCCESS. Geophysical Research Letters 25, 1721–1724.

Tan, D., et al., 2001. HO_x budgets in a deciduous forest: results from the prophet summer 1998 campaign. Journal of Geophysical Research-Atmospheres 106, 24407–24427.

Thompson, A.M., 1992. The oxidizing capacity of the Earth's atmosphere—probable past and future changes. Science 256, 1157–1165.

Wang, Y.H., et al., 2001. Factors controlling tropospheric O_3, OH, NO_x and SO_2 over the tropical Pacific during PEM-Tropics B. Journal of Geophysical Research–Atmospheres 106, 32733–32747.

Yang, J., et al., 2002. Impacts of snowpack emissions on deduced levels of OH and peroxy radicals at Summit. Greenland 15–16, 2523–2534.

Zhou, X., et al., 2001. Snowpack photochemical production of HONO: a major source of OH in the Arctic boundary layer in springtime. Geophysical Research Letters 28, 4087–4090.